Nuclear Engineering and Technology 52 (2020) 2078–2084

Contents lists available at ScienceDirect

Nuclear Engineering and Technology

journal homepage: www.elsevier.com/locate/net

Original Article

Physical and nuclear shielding properties of newly synthesized magnesium oxide and zinc oxide nanoparticles

M. Rashad [a, b], H.O. Tekin [c, *], Hesham MH. Zakaly [d, e], Mariia Pyshkina [d, f], Shams A.M. Issa [a, e], G. Susoy [h]

[a] Nanotechnology Research Laboratory, Department of Physics, Faculty of Science, University of Tabuk, Tabuk, Saudi Arabia
[b] Physics Department, Faculty of Science, Assiut University, 71516, Assiut, Egypt
[c] Medical Diagnostic Imaging Department, College of Health Sciences, University of Sharjah, Sharjah, 27272, United Arab Emirates
[d] Institute of Physics and Technology, Ural Federal University, Yekaterinburg, Russia
[e] Physics Department, Faculty of Science, Al-Azhar University, Assiut, 71452, Egypt
[f] Institute of Industrial Ecology UB RAS, Ekaterinburg, Russia
[h] Istanbul University, Faculty of Science, Department of Physics, Istanbul, 341342, Turkey

ARTICLE INFO

Article history:
Received 6 December 2019
Received in revised form
24 January 2020
Accepted 14 February 2020
Available online 24 February 2020

Keywords:
Zno NPs
MgO NPs
SEM
FLUKA
Shielding

ABSTRACT

Magnesium oxide (MgO) and Zinc oxide (ZnO) nanoparticles (NPs) have been successfully synthesized by solid–solid reaction method. The structural properties of ZnO and MgO NPs were studied using X-ray diffraction (XRD) and scanning electron microscopy (SEM). XRD results indicated a formation of pure MgO and ZnO NPs. The mean diameter values of the agglomerated particles were around to be 70 and 50 nm for MgO and ZnO NPs, respectively using SEM analysis. Further, a wide-range of nuclear radiation shielding investigation for gamma-ray and fast neutrons have been studied for Magnesium oxide (MgO) and Zinc oxide (ZnO) samples. FLUKA and Microshield codes have been employed for the determination of mass attenuation coefficients (μ_m) and transmission factors (TF) of Magnesium oxide (MgO) and Zinc oxide (ZnO) samples. The calculated values for mass attenuation coefficients (μ_m) were utilized to determine other vital shielding properties against gamma-ray radiation. Moreover, the results showed that Zinc oxide (ZnO) nanoparticles with the lowest diameter value as 50 nm had a satisfactory capacity in nuclear radiation shielding.

1. Introduction

MgO is one of the interesting metal oxides that are commonly used when it comes to industrial applications i.e heating apparatus, refractory materials and infrared optics etc. [1,2]. Its band gap is attractive because of its wide like insulator [3]. It is crystallized in cubic Fm-3m space group. Currently, many studies have been done on the synthesis and applications of MgO. Examples of these studies are hydrothermal, sol-gel, flame spray pyrolysis, combustion and aqueous wet chemical, chemical gas phase deposition, and solid-soild reaction [4–9]. ZnO is one of the most popular materials widely used in medical and industrial applications. It is sometimes it is referred to as a bewitched material due to its wide applications range and elasticity of preparation in various morphologies with particular properties [10]. As mention before, ZnO and MgO NPs were used for different applications, but in radiation shielding they have less used in this form, there, these types of pure nanoparticle have an attractive for the scientists in the field of radiation shielding. This branch is considered as an issue that needs to be addressed. It is well-known that nuclear research laboratories, number of nuclear power plants, medical radiation facilities for diagnostic and treatment applications in the medical field are increasing in global World. On the other hand, different types of nanoparticles have been utilized as additive material for development of nuclear shielding performance of ordinary materials. Previously, Mesbahi and Ghiasi [11] studied the nuclear shielding properties of ordinary concrete doped with different types of additives such as H_4B, Fe_2O_3, WO_3, PbO_2 in micro and nano scales. Their results have shown that ordinary concrete with nano-sized particles demonstrated better gamma and neutron shielding performance than micro-sized additives. In another study, Verdipoor et al. [12], the photon mass attenuation coefficients for a silicon resin charged with WO_3, PbO, and Bi_2O_3

* Corresponding author.
E-mail address: tekin765@gmail.com (H.O. Tekin).

https://doi.org/10.1016/j.net.2020.02.013

micro and nano-particles for radiation shielding were investigated. According to their results, the attenuation property of PbO and Bi_2O_3 nanoparticles is higher than WO3 nanoparticles in the energy range examined. To evaluate the performance of WO_3 nanoparticles doped ordinary concrete, Tekin et al. [13], have used MCNPX Monte Carlo code. According to the results of the mass attenuation coefficients, nano-WO_3 doped concrete significantly increases the shielding properties than micro-WO_3. Finally, in the study examined by Tekin et al. [14], gamma radiation shielding features of hematite-serpentine concrete collated with WO_3 and Bi_2O_3 micro and nano particles were investigated. Their results have shown that shielding properties of hematite-serpentine concrete with Bi_2O_3 nano particles was higher than that of corresponding WO_3 mixtures. Overall, literature review showed that using of nanoparticles in advanced material science [15] has a major importance especially in nuclear shielding materials. Therefore, this study has focused on fabrication of two different nano particles and investigates their nuclear radiation shielding properties. First, magnesium oxide (MgO) and zinc oxide (ZnO) nanoparticles (NPs) have been successfully synthesized by solid–solid reaction method. The structural features of ZnO and MgO NPs were studied using X-ray diffraction (XRD) and scanning electron microscopy (SEM). XRD results showed the formation of pure MgO and ZnO NPs. Next, FLUKA and MicroShield codes have been employed for determination of mass attenuation coefficients and transmission factors (TF) of Magnesium oxide (MgO) and Zinc oxide (ZnO) samples. We shall explain experimental procedure and other technical details of present investigation in further parts of this report. It should be noted that the results of this new investigation will be useful in the material science literature for future applications of ZnO and MgO NPs, and particularly their shielding applications in radiation facilities. According to the results of the present study, the role of grain size and the effect of the nanoparticles examined on the nuclear shielding performance will be more clearly understood. Also, obtained results of the present investigation on ZnO and MgO can be utilized for further investigations on development of shielding performances of traditional shielding materials.

2. Preparation method

Solid reaction technique is used to prepare ZnO and MgO NPs at room temperature [15]. 0.2 mol of $ZnCl_2.2H_2O$) and 0.5 mol of NaOH were added in a crucible. The product is steadily converted the ZnO NPs 10 min. Finally, it is washed using distilled water. The strategies for preparation MgO NPs is the pervious one by starting material of $MgCl_2.2H_2O$. The chemical reaction for formation of ZnO has two following steps:

$$ZnCl_2 + 2NaOH = Zn(OH)_2 + 2NaCl \quad (1)$$

$$Zn(OH)_2 \overset{heating}{\rightarrow} ZnO + H_2O \quad (2)$$

2.1. FLUKA

FLUKA (FLUktuierende KAskade) [16,17] is a Monte Carlo simulation code used to record the transportation of about 60 particles and rays e.g. electrons, protons, photons, neutrinos and others, in the substance developed in cooperation between CERN

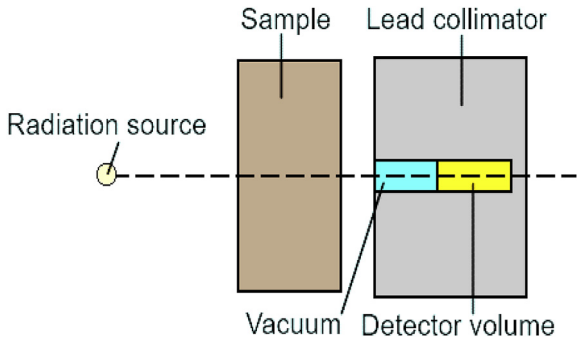

Fig. 2. Sketch of MicroShield simulated geometry for photon attenuation.

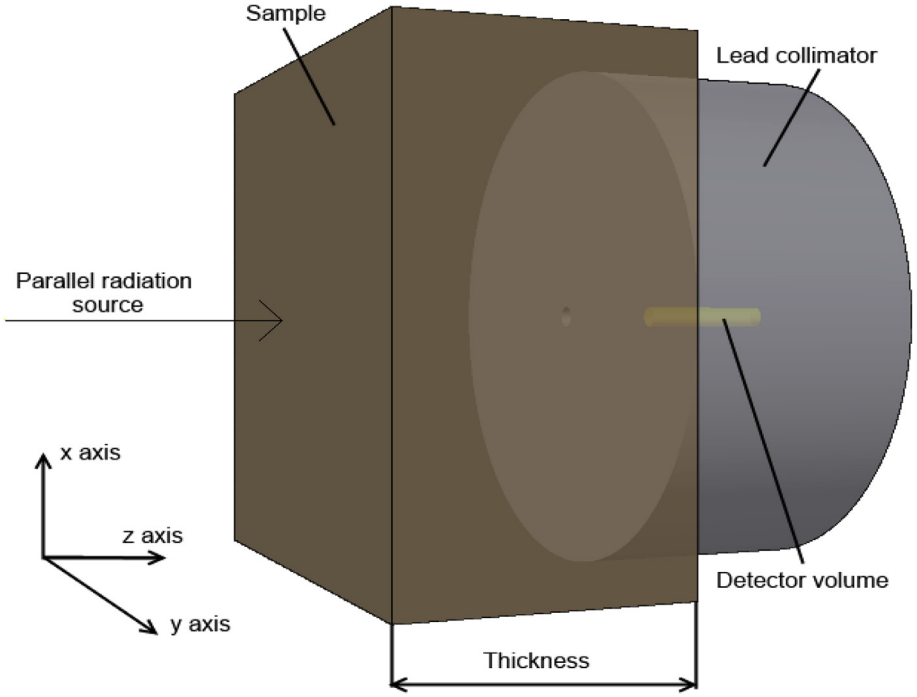

Fig. 1. Sketch of FLUKA simulated geometry for photon attenuation.

(European Council for Nuclear Research) and INFN (Istituto Nazionale di Fisica Nucleare). FLUKA is used in a wide field of research: from the astrophysics up to dosimetry. In this work, FLUKA is used to evaluate the mass attenuation coefficient of the proposed sample. The sample was identified by a MATERIAL card inserted with the necessary COMPOUND cards to describe the requested sample. The MATERIAL card used to identify the chosen composition includes the material number, compound name, and its density, etc. The photon fluence inside the detector volume has been scored with the USRBIN card. The particle type and its energy are described in a BEAM card. In this work, the beam direction, sample, and detector are placed along the z-axis. A beam of 10^5 photons with different energies: from 100 up 1330 keV - has been directed on the sample. The sample has been performed with RPP body. Photons after passing the sample have been detected in detector volume, covered with lead collimator in the case to prevent the

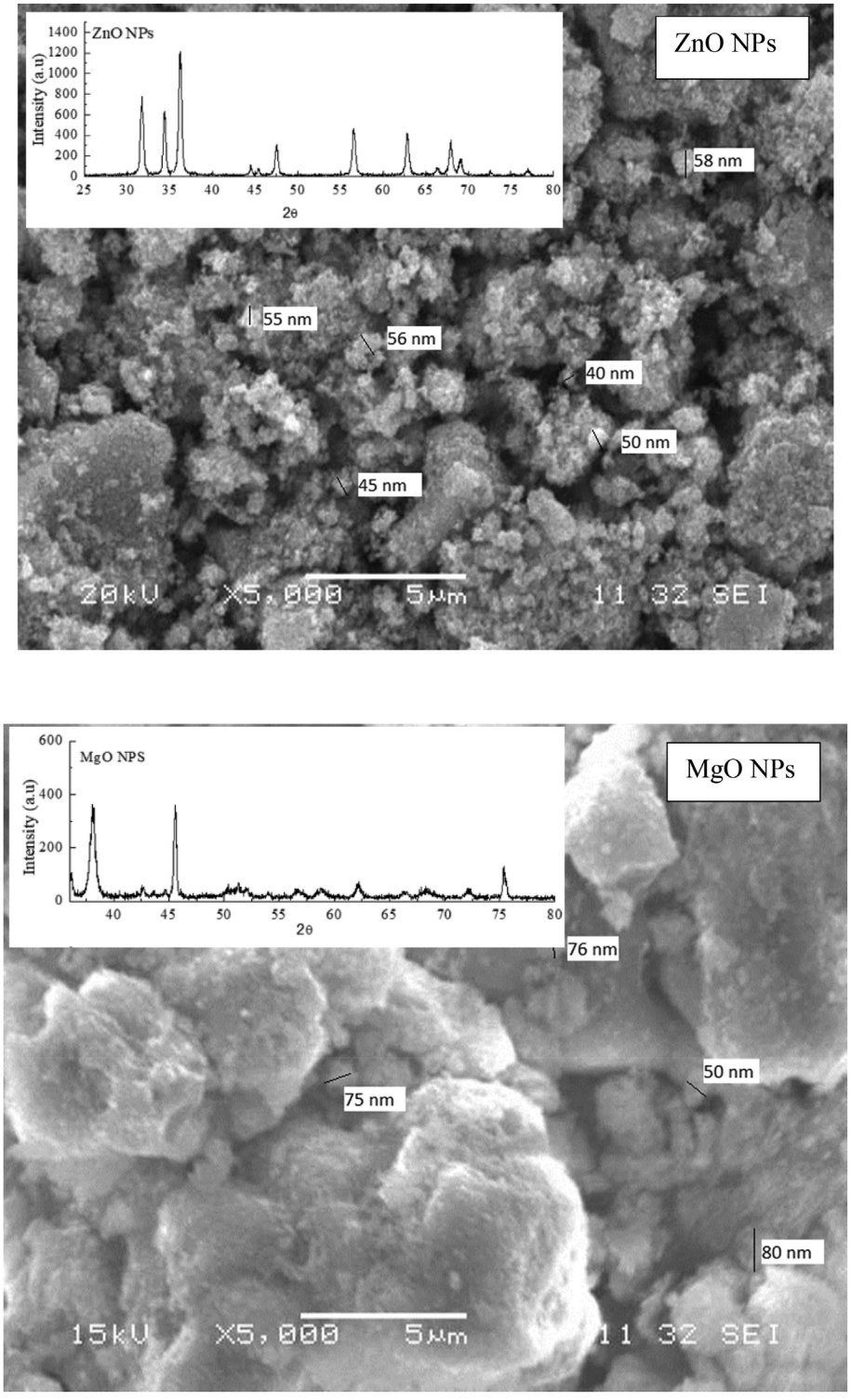

Fig. 3. SEM images of ZnO and MgO NPs (insert Fig. XRD of ZnO and MgO NPs.).

detection of scattered photons (Fig. 1). A well geometry condition was fulfilled by two uniform collimators with 0.15 cm gap radius. Thus, the detection field was prevented from the interactions of scattered photons. Further, the rest of simulation environment was filled with vacuum.

2.2. MicroShield

Microshield [18] is a universal photon/gamma-ray shielding and dose assessment program. It has a user-friendly interface and ability to work with sources of different geometries and with shielding of complex compound. The certain material compound might be created with Microshield and its main characteristics like mass and linear attenuation coefficient, mean free path, etc. might be distinguished as well. In this work the sample material has been created with Microshield using the density and composition. The mass attenuation coefficient has been obtained (Fig. 2).

3. Results and discussion

3.1. SEM results

ZnO and MgO NPs morphologies using SEM were illustrated in Fig. 3. It tends that, ZnO and MgO NPs have semi-spherical figure with some agglomerated particles. Using these SEM images, the of them were calculated which are 50 and 70 nm for ZnO and MgO NPs, respectively. Fig. 3 has been marked for identifying the grain size which calculated using *Image J* program [19].

3.2. XRD results

XRD results of ZnO and MgO NPs are presented in insert Fig. 3. For both NPs, the diffraction peaks position relating to the crystal planes for ZnO NPs and MgO NPs are hexagonal and cubic structure, respectively [19]. Additionally, peaks at angle of 52, 58 and 68° are denoted to Mg(OH)2.

From XRD results, one can calculate the crystallites size, D, using Scherrer equation [18].

$$D = \frac{K\lambda}{\beta\cos\theta} \tag{3}$$

K~1, λ: wavelength of XRD source and β: full width at half maximum. Important structure parameters could be obtained from XRD results called strain, ε and dislocation density, δ [18]:

$$\varepsilon = \frac{\beta}{4\tan\theta} \tag{4}$$

$$\delta = \frac{1}{D^2} \tag{5}$$

Using the Scherrer equation eq. (1), the calculated values of (D) are 20 nm for ZnO NPs and 25 nm for MgO NPs. These calculated values are comparable to those from SEM results [19]. Moreover, the calculated values of strain for ZnO and MgO NPs are 6.5×10^{-4} and 5×10^{-4}, respectively. On the other hand, the values of dislocation density are 2 × 1015 and 3 × 1015 (line m)$^{-2}$ for ZnO and MgO NPs, respectively.

3.3. Radiation shielding properties of MgO and ZnO samples

In this study, gamma transmission (TF) ratios of the investigated ZnO and MgO samples were determined for photon energies of 0.356, 0.662, 1.173 and 1.330 MeV. The variations of the transmission factors (TF) according to sample thickness are shown in Fig. 4 and Fig. 5, respectively. As the thickness of the examined samples increases, the TF values decrease rapidly and the lowest diameter (50 nm) ZnO nanoparticle has the smallest TF values in all energy values compared to the MgO sample. This means that for larger energies the material thickness needs to be increased. The values of linear attenuation coefficients (μ) for the examined samples are compared and presented in Fig. 6. A sharp decrease in the linear attenuation coefficients of the studied samples against the photon energy was obtained.

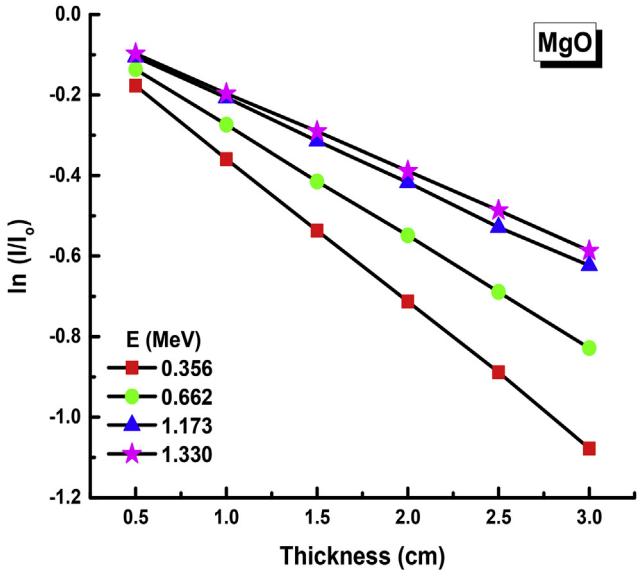

Fig. 4. Variation of transmission photon flux as a function of sample thicknesses.

The figure displays that a dramatic decrease in the linear attenuation coefficients of the investigated samples against photon energy has obtained. On the other hand, it can be also seen from Fig. 6 that linear attenuation coefficients of ZnO were higher than MgO in all photon energies. This can be due the higher gamma attenuation properties of ZnO than MgO due to the differences in the obtained mean diameters. Similar results about the relationship between gamma attenuation properties and additive grain size

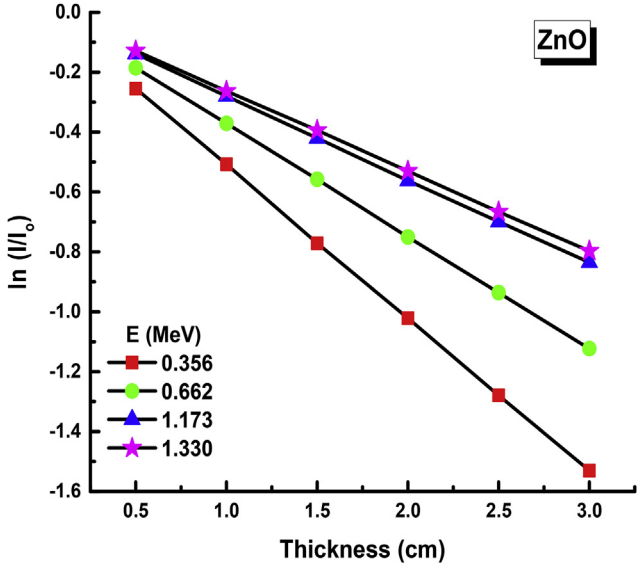

Fig. 5. Variation of transmission photon flux as a function of sample thicknesses.

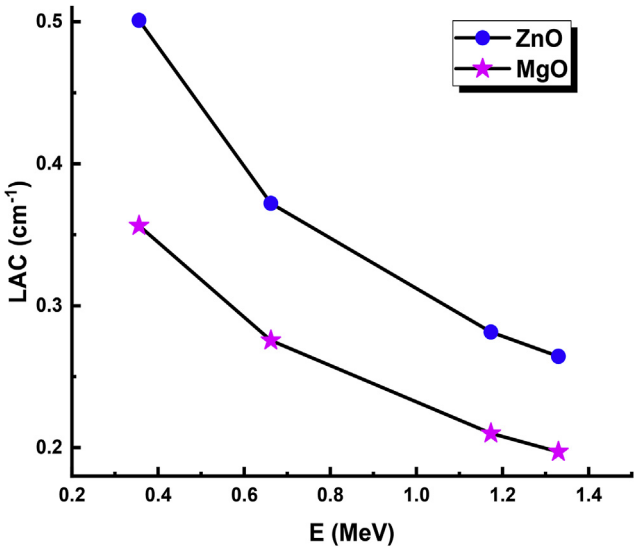

Fig. 6. Linear attenuation coefficient (LAC) values for investigated samples against photon energy.

Table 1
Mass attenuation coefficient using Microshield, FLUKA and their relative difference (RD) at deferent photon energy.

Energy (MeV)	ZnO		
	MicroShield	FLUKA	RD
0.356	0.0983	0.0999	1.63
0.662	0.0731	0.0728	0.41
1.173	0.0558	0.0543	2.69
1.330	0.0523	0.0505	3.44
Energy (MeV)	**MgO**		
	MicroShield	**FLUKA**	**RD**
0.356	0.0995	0.0984	1.11
0.662	0.0769	0.0763	0.78
1.173	0.0590	0.0584	1.02
1.330	0.0553	0.0545	1.45

$$RD = \left(\frac{MicroShield - FLUKA}{MicroShield}\right) \times 100$$

have reported by Tekin et al. [13]. Table 1 presents the mass attenuation coefficient using Microshield, FLUKA and their relative difference (RD) at deferent photon energy. The important parameters for determining the thickness of the material at the selected photon energies and also for determining the shielding effect of the material are the average free path (MFP), the half value layer and tenth value layer (HVL and TVL). Low HVL, TVL and MFP values indicate superior shielding capability [20–25]. These values, which show similar variations with each other [26–29], are shown in Figs. 7–9 against photon energy, respectively. As seen from Figs. 7, 8 and 9, it is clear that the HVL, TVL and MFP values of the ZnO and MgO samples increase as photon energy increases. They reach the maximum for ZnO and MgO samples at 1.33 MeV. Also, ZnO with the lowest particle diameter has been found as superior material to decrease the MFP, HVL and TVL and increase the gamma attenuation capability. There is also an inverse relationship between grain size and HVL, TVL and MFP values. Fig. 10 shows the neutron absorption parameters (absorption neutron scattering cross section (σ_{abs})) in the ZnO and MgO, relatively. As can be seen from the figure, σ_{abs} values increase as the nanoparticle diameter decreases. It is known that the material having maximum neutron absorption parameters (σ_{abs}) is more suitable for neutron shielding. Thus, the ZnO sample has the largest neutron absorption parameter. Therefore, it can be said that ZnO sample has better neutron shielding properties with it's lower particle diameter.

4. Conclusion

The preparations of ZnO and MgO NPs have been done using solid reaction technique. XRD confirm the formation of both ZnO and MgO NPs. The 50 and 70 nm agglomerated grain size were calculated using SEM images. The importance of the nanoparticles for different types of applications is increasing day-by-day. Thus, the aim of the advanced investigations such as determination of structural, physical and chemical properties of different type nanoparticles is significant. Considering the importance of those investigations, solid–solid reaction method is used for preparing the MgO and ZnO NPs. XRD confirm the formation of both MgO and ZnO NPs. SEM images shows the surface morphology of MgO and ZnO NPs which show agglomerated particles of 50 and 70 nm. Also, nuclear shielding performance of MgO and ZnO has been

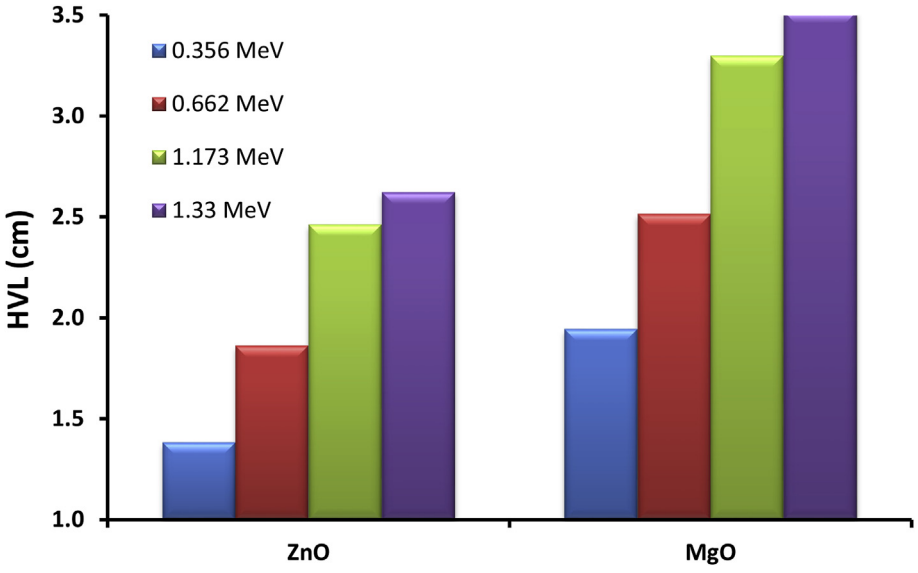

Fig. 7. Variation of HVL for investigated samples.

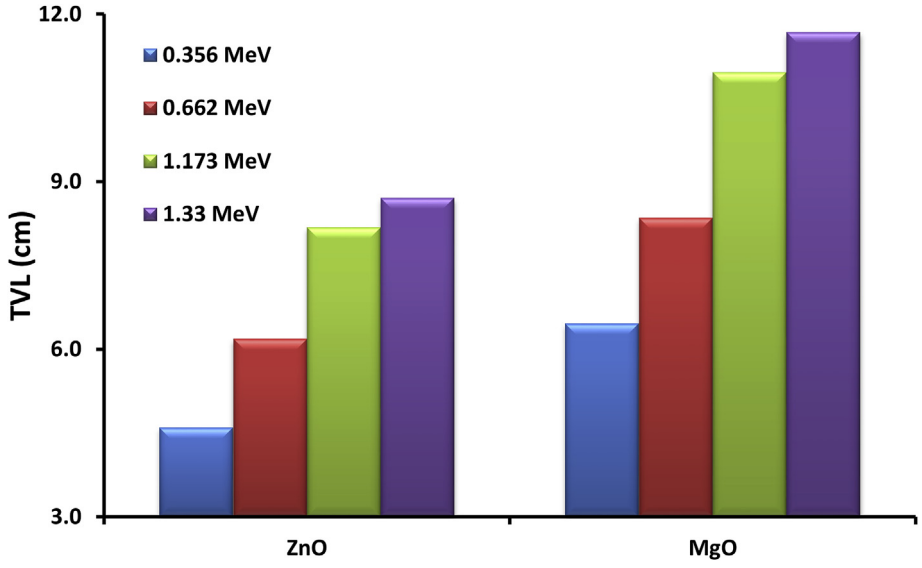

Fig. 8. Variation of TVL for investigated samples.

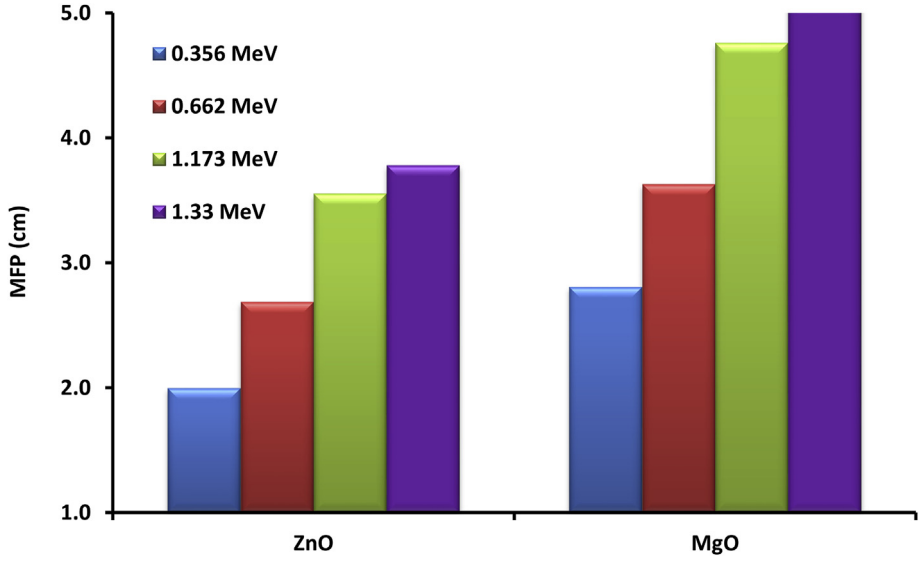

Fig. 9. Variation of MFP for investigated samples.

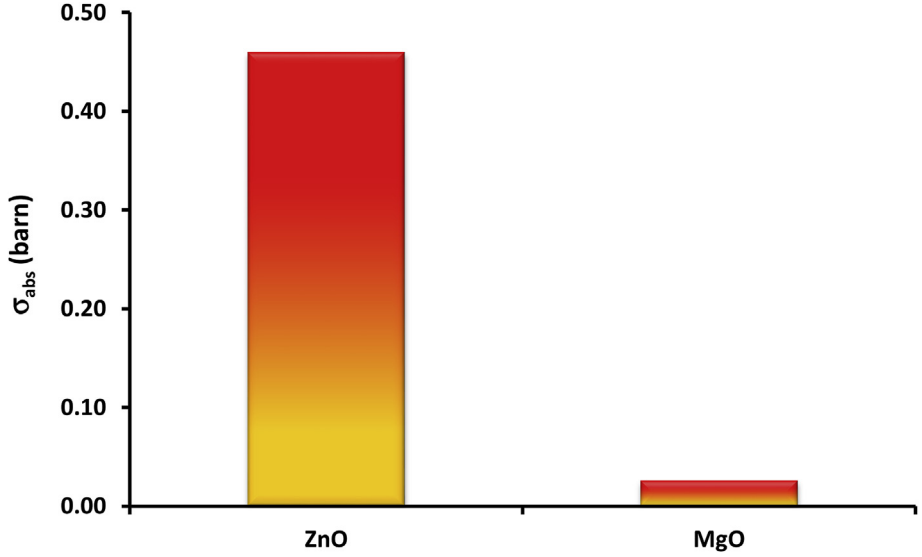

Fig. 10. Absorption neutron scattering cross section (σ_{abs}) for investigated samples.

investigated. The hypothesis of this study was to evaluate the relationship between grain size and shielding efficiency of investigated materials. The results have showed that grain size has a significant impact on shielding performance. The ZnO nanoparticle with lower grain size provided better shielding properties. In addition, Previous studies also reported the similar behaviors of different types of additive nanoparticles in shielding materials. It can be concluded from this study that MgO and ZnO NPs can be further investigated as additive material in ordinary shielding materials as well as in alloys and glassy systems.

Declaration of competing interest

There are no conflicts of interest to declare.

References

[1] L.A. Ma, Z.X. Lin, J.Y. Lin, Y.A. Zhang, L.Q. Hu, T.L. Guo, Large-scale growth of ultrathin MgO nanowires and evaluate their field emission properties, Physica E 41 (8) (2009) 1500–1503, https://doi.org/10.1016/j.physe.2009.04.028.

[2] Vipin Kumar, M.K. Sharma, J. Gaur, T.P. Sharma, Polycrystalline ZnS thin films by screen printing method and its characterization, Chalcogenide Lett. 5 (November 2008) 289–295.

[3] A.M.E. Raj, V.B. Jothy, C. Ravidhas, T. Som, M. Jayachandran, C. Sanjeeviraja, Effect of embedded lithium nanoclusters on structural, optical and electrical characteristics of MgO thin films, Radiat. Phys. Chem. 78 (2009) 914–921.

[4] A. Kumar, J. Kumar, On the synthesis and optical absorption studies of nano-size magnesium oxide powder, J. Phys. Chem. Solid. 69 (2008) 2764–2772.

[5] T. Selvamani, T. Yagyu, S. Kawasaki, I. Mukhopadhyay, Easy and effective synthesis of micrometer-sized rectangular MgO sheets with very high catalytic activity, J. Catal. Commun. 11 (2010) 537–541, https://doi.org/10.1016/j.catcom.2009.12.014.

[6] J. Jiu, K.I. Kurumada, M. Tanigaki, Preparation of nanoporous silica using copolymer template, Mater. Chem. Phys. 78 (2002) 177–183, https://doi.org/10.1016/S0254-0584(02)00340-1.

[7] A.V. Chadwick, I.J.F. Poplett, D.T.S. Maitland, M. E Smith, Oxygen speciation in nanophase MgO from solid-state 17O NMR, Chem. Mater. 10 (1998) 864–870, https://doi.org/10.1021/cm970629+.

[8] X. Bokhimi, A. Morales, M. Portilla, A. Garcıa-Ruiz, Hydroxides as precursors of nanocrystalline oxides, Nanostruct. Mater. 12 (1999) 589–592.

[9] A. Subramania, G.V. Kumar, A.R. Priya, T. Vasudevan, Polyol-mediated thermolysis process for the synthesis of MgO nanoparticles and nanowires, Nanotechnology 18 (2007) 1–5, https://doi.org/10.1088/0957-4484/18/22/225601.

[10] A. Khorsand Zak, R. Razali, WH Abd Majid, Majid Darroudi, Int. J. Nanomed. 6 (2011) 1399–1403.

[11] Asghar Mesbahi, Hosein Ghiasi, Shielding properties of the ordinary concrete loaded with micro- and nano-particles against neutron and gamma radiations, Appl. Radiat. Isot. 136 (2018) 27–31, https://doi.org/10.1016/j.apradiso.2018.02.004.

[12] Khatibeh Verdipoor, Abdolali Alemi, Asghar Mesbahi, Photon mass attenuation coefficients of a silicon resin loaded with WO3, PbO, and Bi2O3 Micro and Nano-particles for radiation shielding, Radiat. Phys. Chem. 147 (2018) 85–90, https://doi.org/10.1016/j.radphyschem.2018.02.017.

[13] H.O. Tekin, V.P. Singh, T. Manici, Effects of micro-sized and nano-sized WO3 on mass attenuation coefficients of concrete by using MCNPX code, Appl. Radiat. Isot. 121 (2017) 122–125, https://doi.org/10.1016/j.apradiso.2016.12.040.

[14] H.O. Tekin, M.I. Sayyed, Shams A.M. Issa, Gamma radiation shielding properties of the hematite-serpentine concrete blended with WO3 and Bi2O3 micro and nano particles using MCNPX code, Radiat. Phys. Chem. 150 (2018) 95–100, https://doi.org/10.1016/j.radphyschem.2018.05.002.

[15] Jun-Hua Liu, Quan-Ping Zhang, Nan Sun, Yang Zhao, Rui Shi, Yuan-Lin Zhou, Jian Zheng, Elevated gamma-rays shielding property in lead-free bismuth tungstate by nanofabricating structures 112, 2018, pp. 185–189, https://doi.org/10.1016/j.jpcs.2017.09.007.

[16] Fluka: a multi-particle transport code", A. Ferrari, P.R. Sala, A. Fass`o and J. Ranft, CERN–2005–10 (2005), INFN/TC 05/11, SLAC–R–773

[17] T.T. Böhlen, F. Cerutti, M.P.W. Chin, A. Fass`o, A. Ferrari, P.G. Ortega, A. Mairani, P.R. Sala, G. Smirnov, V. Vlachoudis, The fluka code: developments and challenges for high energy and medical applications, Nucl. Data Sheets 120 (2014) 211–214.

[18] https://www.radiationsoftware.com/microshield.

[19] M. Rashad, Performance efficiency and kinetic studies of water purification using ZnO and MgO nanoparticles for potassium permanganate, Opt. Quant. Electron. 51 (2019) 291.

[20] H.O. Tekin, E. Kavaz, E.E. Altunsoy, M. Kamislioglu, O. Kilicoglu, O. Agar, M.I. Sayyed, Nevzat Tarhan, Characterization of a broad range gamma-ray and neutron shielding properties of MgO-Al2O3-SiO2-B2O3 and Na2O-Al2O3-SiO2 glass systems, J. Non-Cryst. Solids 518 (2019) 92–102, https://doi.org/10.1016/j.jnoncrysol.2019.05.012.

[21] H.O. Tekin, E. Kavaz, Athanasia Papachristodoulou, M. Kamislioglu, O. Agar, E.E. Altunsoy Guclu, O. Kilicoglu, M.I. Sayyed, Characterization of SiO2–PbO–CdO–Ga2O3 glasses for comprehensive nuclear shielding performance: alpha, proton, gamma, neutron Radiation, Ceram. Int. 45 (2019) 19206–19222, https://doi.org/10.1016/j.ceramint.2019.06.168.

[22] Shams A.M. Issa, H.O. Tekin, The multiple characterization of gamma, neutron and proton shielding performances ofxPbO-(99-x)B2O3–Sm2O3 glass system, Ceram. Int. (7 August 2019), https://doi.org/10.1016/j.ceramint.2019.08.065.

[23] Shams A.M. Issa, H.O. Tekin, T.T. Erguzel, G. Susoy, The effective contribution of PbO on nuclear shielding properties of xPbO-(100 – x)P2O5 glass system: a broad range investigation, Appl. Phys. A 125 (2019) 640, https://doi.org/10.1007/s00339-019-2941-x.

[24] H.O. Tekin, L.R.P. Kassab, Shams A.M. Issa, C.D.S. Bordon, E.E. Altunsoy Guclu, G.R. da Silva Mattos, Ozge Kilicoglu, Synthesis and nuclear radiation shielding characterization of newly developed germanium oxide and bismuth oxide glasses, Ceram. Int. (22 August 2019), https://doi.org/10.1016/j.ceramint.2019.08.204.

[25] Ozge Kilicoglu, H.O. Tekin, Bioactive glasses and direct effect of increased K2O additive for nuclear shielding performance: a comparative investigation, Ceram. Int. (11 September 2019), https://doi.org/10.1016/j.ceramint.2019.09.095.

[26] Shamsan S. Obaid, Dhammajot K. Gaikwad, Pravina P. Pawar, Determination of gamma ray shielding parameters of rocks and concrete, Radiat. Phys. Chem. 144 (2018) 356e360, https://doi.org/10.1016/j.radphyschem.20.

[27] V.V. Awasarmol, D.K. Gaikwad, Shamsan S. Obaid, P.P. Pawar, Gamma radiation studies on organic nonlinear optical materials in the energy range 122e1330 keV, Proc. Natl. Acad. Sci. India Sect. A (Phys. Sci.): Phys. Sci. 1e6 (2019), https://doi.org/10.1007/s40010-019-00636-1.17.09.022.

[28] D.K. Gaikwad, M.I. Sayyed, S.N. Boteward, Shamsan S. Obaid, Z.Y. Khattari, U.P. Gawai, Feras Afsaneh, M.D. Shirshat, P.P. Pawar, Physical, structural, optical investigation and shielding features of tungsten bismuth tellurite based glasses, J. Non-Cryst. Solids 503 (2019) 158e168, https://doi.org/10.1016/j.jnoncrysol.2018.09.038.

[29] Shamsan S. Obaid, M.I. Sayyed, D.K. Gaikwad, H.O. Tekin, Y. Elmahrough, P.P. Pawar, Photon attenuation coefficients of different rock samples using MCNPX, Geant4 simulation codes and experimental results: a comparison study, Radiat. Eff. Defect Solid 173 (2018), 11e12, https://doi.org/10.1080/10420150.2018.1505890, 900-914.